View metadata, citation and similar papers at core.ac.uk

brought to you by CORE

provided by Repository@Nottingham

Polymer 55 (2014) 321–325

Contents lists available at SciVerse ScienceDirect

Polymer

journal homepage: www.elsevier.com/locate/polymer

Post-synthetic modification of conjugated microporous polymers☆

Thanchanok Ratvijitvech [a], Robert Dawson [a], Andrea Laybourn [a], Yaroslav Z. Khimyak [b], Dave J. Adams [a,*], Andrew I. Cooper [a,*]

[a] Department of Chemistry and Centre for Materials Discovery, University of Liverpool, Liverpool L697ZD, UK
[b] School of Pharmacy, University of East Anglia, Norwich Research Park, Norwich NR4 7TJ, UK

ARTICLE INFO

Article history:
Received 9 May 2013
Received in revised form
4 June 2013
Accepted 5 June 2013
Available online 14 June 2013

Keywords:
Microporous
Polymer synthesis
Conjugated polymer

ABSTRACT

Control over the surface functionality and microporosity in conjugated microporous polymers (CMPs) has been achieved by the post-synthetic modification of amines into amides of with different alkyl chains, one of which was chiral. The surface areas, pore volumes, carbon dioxide uptakes and isosteric heat of adsorption for carbon dioxide can be rationally tuned.

© 2013 The Authors. Published by Elsevier Ltd. All rights reserved.

1. Introduction

Microporous organic polymers (MOPs) [1–3] are attracting much interest currently because of their potential uses in catalysis [4], gas storage [5], carbon dioxide capture [6–8], light harvesting and photoluminescence [9–11], electrical energy storage [12], and separation [13]. MOPs have potential advantages over many other microporous materials because of the scope of synthetic diversity [1–3,14–16], the attainment of ultrahigh surface areas [17–19], and high physicochemical stabilities, especially towards water [17,19]. MOP-forming reactions tend to involve mild synthetic conditions, which allows the incorporation of pendant functionalities such as amines and alcohols [15,16] while maintaining high thermal stabilities in the materials (up to around 500 °C) [11,17]. Such functionalisation can prove more difficult in other materials, such as metal-organic frameworks (MOFs), since polar groups such as amines and acids can coordinate to the metal centres or be incompatible with solvothermal reaction conditions [20]. One subclass of MOPs, known as conjugated microporous polymers (CMPs), are formed using metal-catalysed cross-coupling chemistry, such as the palladium-catalysed Sonogashira–Hagihara reaction, to form networks with extended conjugation [21]. CMPs can have apparent Brunauer–Emmett–Teller (BET) surface areas greater than 1000 m^2/g [22], and the average pore size in the amorphous networks can be tuned by varying the strut lengths of the monomers [23]. We and others have shown that this type of chemistry is suitable for the formation of networks containing a wide range of functional groups [15,24,25].

The incorporation of new functional groups into MOFs by post-synthetic modification (PSM) [20,26,27] has led to new functional materials that can incorporate, for example, catalytic centres [28]. While there are a number of reports of PSM in MOFs [26,27], there are few examples within the MOP literature [29–35]. Polymers of intrinsic microporosity (PIMs) have been post-functionalised by chemical hydrolysis of the pendant nitrile functionalities in the soluble polymer PIM-1 to produce carboxylic acids [31,32]. Likewise, reactions with NaN_3 forms tetrazole rings, and the derivatized PIM shows increased selectively for the separation of CO_2/N_2 [29]. An imine-based covalent organic framework (COF-300) has also been post-synthetically modified by reduction of the imine bond to an amine, followed by a reaction with acetic anhydride to form an amide [30]. However, after reduction, the network did not maintain its porosity. CMPs and COFs have been post-functionalised by thiol-yne and thiol-ene chemistry, reacting at the alkyne groups of the CMP or onto alkene groups on a COF [34–36] We have also post-metallated bypridyl-containing CMPs to form metal-organic CMPs (MO-CMPs) which have some resemblance to MOFs and which can show catalytic activity [33].

Here, we report the post-synthetic modification of an amine-functionalised CMP (**CMP-1-NH_2**) [7] by reaction with a series of anhydrides to produce amide-functionalised networks that retain microporosity. We also explore the effect of the modification on the

☆ This is an open access article under the CC BY license (http://creativecommons.org/licenses/by/3.0/).

* Corresponding authors.
E-mail addresses: d.j.adams@liverpool.ac.uk (D.J. Adams), aicooper@liv.ac.uk (A.I. Cooper).

0032-3861/$ – see front matter © 2013 The Authors. Published by Elsevier Ltd. All rights reserved.
http://dx.doi.org/10.1016/j.polymer.2013.06.004

pore structure of the networks, as well as demonstrating that the method opens up routes to new properties in MOPs, for example the introduction of chirality.

2. Experimental

2.1. Materials

1,3,5-Triethynylbenzene and tetrakis(triphenylphosphine) palladium(0) were purchased from Alfa-Aesar. All other chemicals were purchased from Sigma–Aldrich with a purity of 97% or greater.

3. Methods

3.1. Gas sorption

All samples were heated to 120 °C for at least 12 h under dynamic vacuum before each gas sorption measurement. Nitrogen gas sorption was performed using a Micromeritics ASAP 2020 instrument at a temperature of 77.3 K. BET surface areas were calculated over the relative pressure range 0.05–0.15 P/P_0. Total pore volumes were measured at 0.99 P/P_0, while microporosity was estimated by measuring the pore volume at a relative pressure of 0.1 P/P_0. Differential pore volumes were calculated using the NLDFT cylindrical pore model for pillared clay, which was found to give the lowest standard deviations when used for other CMP materials. CO_2 isotherms were measured at 273 K using a Micromeritics 2020 volumetric adsorption analyser. Temperatures were controlled using a chiller/circulator. CO_2/N_2 selectivies were calculated using the Henry's law constants method by measuring the slopes of the isotherms [37].

3.2. Infra-red spectra

IR spectra were measured on a Bruker Tensor 27 using pressed KBr discs.

3.3. Solid-state NMR

Solid-state NMR spectra were measured using a Bruker Avance 400 DSX spectrometer operating at 100.61 MHz for ^{13}C and 400.13 MHz for ^{1}H. $^{1}H-^{13}C$ cross-polarisation magic angle spinning (CP/MAS) NMR experiments were carried out at an MAS rate of 10 Hz using zirconia rotors 4 mm in diameter. The ^{1}H $\pi/2$ pulse was 3.4 μs, and two-pulse phase modulation (TPPM) decoupling was used during the acquisition. The Hartmann–Hahn condition was set using hexamethylbenzene. The spectra were measured using a contact time of 2.0 ms and a relaxation delay of 10.0 s. Typically, 3072 scans were accumulated. The values of the chemical shifts are referred to that of TMS. The analysis of the spectra (deconvolution and integration) were carried out using Bruker TOPSPIN software.

3.4. Synthesis of **CMP-1-NH$_2$** network

1,3,5-Triethynylbenzene (600 mg, 4 mmol) and 2,5-dibromoaniline (1003 mg, 4 mmol) were added to a 100 mL Radleys reaction flask fitted with a condenser and magnetic stirrer. The flask was evacuated and backfilled with nitrogen three times before anhydrous *N*,*N*′-dimethylformamide (6 mL) and anhydrous triethylamine (6 mL) were added via a syringe. The solution was then heated to 100 °C and tetrakis(triphenylphosphine)palladium(0) (200 mg) and CuI (60 mg) were added as a slurry in *N*,*N*′-dimethylformamide (2 mL). The reaction was stirred at 100 °C under nitrogen for 24 h after which the solid precipitate was washed with hot *N*,*N*′-dimethylformamide and Soxhlet extracted with methanol for 18 h. The insoluble brown powder was dried under vacuum at 70 °C for at least 12 h. Yield: 861 mg, 90% (theory 956 mg). Microanalysis: C 78.18%, H 3.59%, N 2.62%.

3.5. Post-synthetic modification of **CMP-1-NH$_2$** to **CMP-1-AMD**

CMP-1-NH$_2$ (119 mg, 0.5 mmol) was stirred in the neat anhydride (2 mL) for 24 h at 30 °C, after which the solid was filtered off and washed with $CHCl_3$ to obtain brown powder. The product was then dried in vacuo at 70 °C for at least 12 h. Yield: 65–85%.

4. Results and discussion

CMP-1-NH$_2$ was reported previously by our group [7] and was formed by the Sonogashira–Hagihara palladium cross-coupling reaction of 1,3,5-triethynylbenzene with 2,5-dibromoaniline (Scheme 1).

Here, the network was re-synthesised, but on a larger scale than that previously reported. The porosity of the network was characterised by nitrogen gas adsorption/desorption at 77 K (Fig. 1). Large amounts of nitrogen were adsorbed at low pressures, indicative of adsorption into micropores, after which further filling of the larger micropores and mesopores was observed. **CMP-1-NH$_2$** showed a hysteresis upon desorption, as reported previously [7]. The apparent BET surface area of the network was calculated to be 656 m^2/g over a relative pressure (P/P_0) range of 0.05–0.15, comparable to that previously reported on a smaller scale (710 m^2/g) [26]. The total pore volume of the network (V_{tot}) calculated at $P/P_0 = 0.99$ to be 0.41 cm^3/g. The pore volume at $P/P_0 = 0.1$ ($V_{0.1}$) was used as a qualitative measure of the degree of microporosity, and was calculated for **CMP-1-NH$_2$** to be 0.25 cm^3/g. The micropore volume as a fraction of the total pore volume ($V_{0.1/tot}$) was therefore calculated to be 0.61. These pore volumes are very close to the smaller scale which has $V_{tot} = 0.39$, $V_{0.1} = 0.24$ and $V_{0.1/tot} = 0.62$.

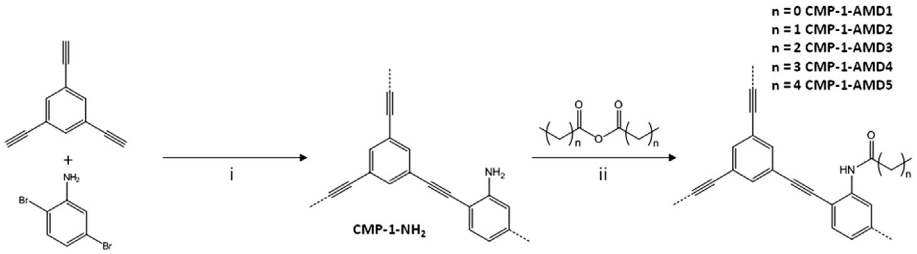

Scheme 1. (i) Synthesis of **CMP-1-NH$_2$**: $Pd(PPh_3)_4$, CuI, DMF, NEt_3, 100 °C, 24 h under N_2 atmosphere. (ii) Post-synthetic modification using anhydrides, $n = 0–4$ & 8 (*i.e.*, $C_1–C_5$ & C_9): 24 h, 30 °C.

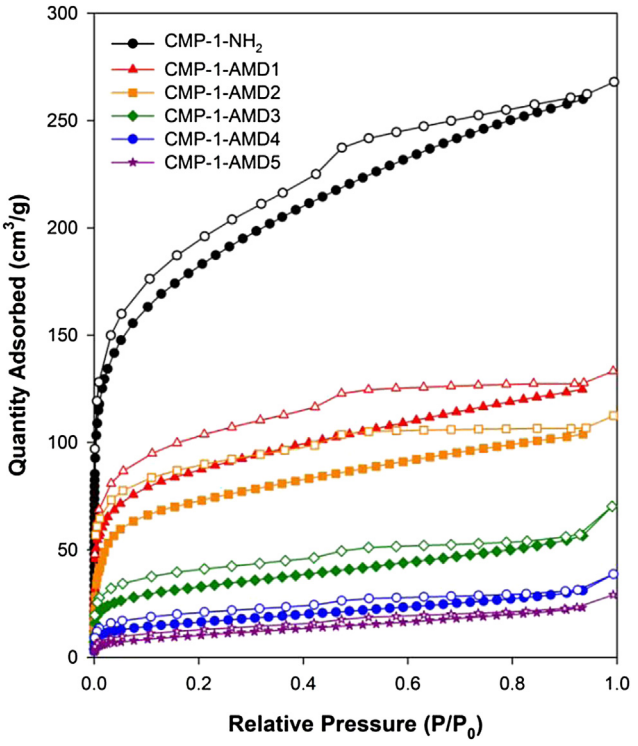

Fig. 1. Nitrogen adsorption (closed symbols)/desorption (open symbols) isotherms for **CMP-1-NH$_2$** and the post-synthetically modified amides, **CMP-1-AMD1**–**CMP-1-AMD5**.

These data demonstrates the efficiency of the synthetic procedure upon scale-up (to 0.86 g of polymer).

The reactivity of the amine functionality in the network was exploited to further functionalise the polymer. Cohen's group have shown that it is possible to post-synthetically modify amino-functionalised MOFs using amidation via reaction with anhydrides [38,39]. Using this methodology, they were able to introduce different functional groups, whilst showing that access to the pores is important for effective modification. Initially, the pendant amine was reacted with acetic anhydride to form **CMP-1-AMD1** (Scheme 1) by simply stirring in neat acetic anhydride for 24 h at 30 °C. The conversion of the amine to amide was confirmed using FT-IR spectroscopy (Fig. 2), which showed the presence of a new band at 1693 cm^{-1}, indicative of an amide carbonyl stretch.

In both spectra, the presence of the internal alkynes as well as a smaller amount of terminal alkyne was observed at *ca.* 2195 and 2108 cm^{-1}, respectively, as shown for previous CMP materials [7]. Elemental analysis showed the nitrogen content was 2.62%, confirming the incorporation **CMP-1-NH$_2$** of amine within the network (Table S1). After post-synthetic modification with acetic anhydride, the nitrogen content decreases to 2.27% due to the presence of the amide group. SEM images of the networks show a rough-textured morphology for both **CMP-1-NH$_2$** and the modified network (see Supporting information; Figs. S12 and S13), implying that amidation does not result in any obvious morphological changes.

The amidation of the network was further confirmed by solid-state ^{1}H–^{13}C CP/MAS NMR for **CMP-1-NH$_2$** and **CMP-1-AMD1** (Fig. 3). Loss of the amine resonance at 144.0 ppm (Fig. 3, bottom) and the presence of additional peaks in the NMR spectrum for **CMP-1-AMD1** (Fig. 3, top) at 23.9 ppm due to the –CH$_3$ carbon in the amide and at 169.2 ppm due to the carbonyl –C=O in the amide group indicate that post-synthetic modification was successful. All other peaks are consistent with previous networks

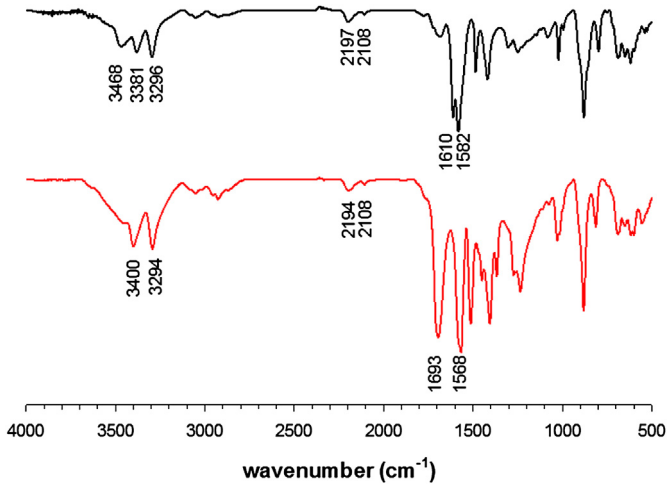

Fig. 2. FT-IR spectra of **CMP-1-NH$_2$** (black) and **CMP-1-AMD1** (red). (For interpretation of the references to colour in this figure legend, the reader is referred to the web version of this article.)

[15,16,23,40,41]. When using an analogous reaction to post-synthetically modify a number of MOFs, Wang et al. showed that the conversion was dependant on the alkyl chain length [38]. This was explained in terms of access of the reagent to the pores. Here, it is more difficult to measure conversions since the polymers cannot be trivially decomposed to small molecules which can be analysed by NMR or HPLC for example, as is the case for MOFs [38]. To probe conversion, we relied on elemental analysis data, which we highlight is difficult. It is known that many microporous polymers give pore data here due to adsorbed gases and water vapour, as well as residual end groups and potentially catalyst residues. As a result, there are many examples where the measured elemental analysis deviates from that expected. Nonetheless, here we have post-functionalised one polymer. Hence, working from the values for the parent polymer, we have estimated the conversions (Table S2, Supporting Information). Here, we find that the conversions are generally approximately 50% for **CMP-1-AMD1** to **CMP-1-AMD5**.

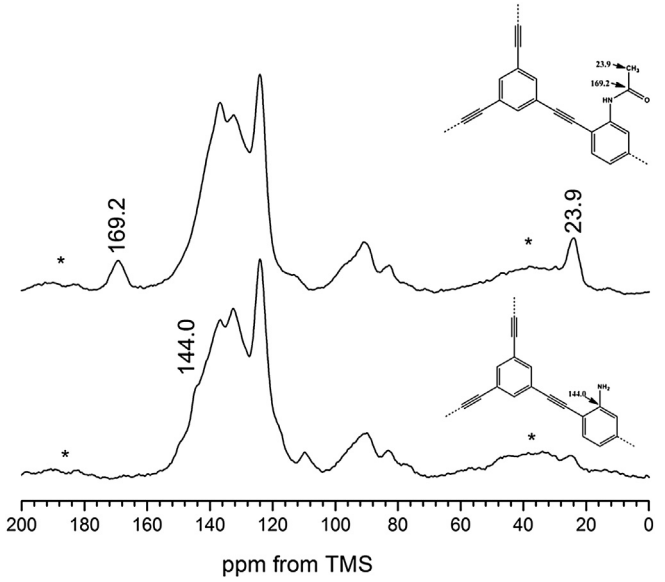

Fig. 3. ^{1}H–^{13}C CP/MAS NMR spectra of **CMP-1-NH$_2$** (bottom) and **CMP-1-AMD1** (top). * Indicate spinning side bands.

Compared to the examples of MOFs [38], the conversion seems less affected by chain length, which may represent the wider pore size distribution of such polymers (see below) as compared to MOFs.

The porosity in **CMP-1-AMD1** was examined using nitrogen adsorption (Fig. 1) and the apparent BET surface area was calculated to be 316 m^2/g, lower than the parent amine network. This decrease in surface area can be attributed to the partial filling of the pores in the network by the amide functionalities, as also reported for MOFs [42]. Similarly, decreases in nitrogen uptake by covalent organic frameworks [43] and polymers of intrinsic microporosity [44] have been reported when the constituents are functionalized by longer alkyl chain. Commensurate with this decrease in surface area, both the total and micropore volumes showed decreases to 0.21 and 0.12 cm^3/g, respectively, while $V_{0.1/tot}$ stayed, within error, the same (0.59). The pore size distribution calculated from the nitrogen adsorption isotherm using the NLDFT cylindrical pore model for pillared clay [16] showed that the pores were centred below 2 nm, and the amide-functionalised material can therefore still be classed as microporous.

To further investigate the effect of the post-synthetic modification on the porosity of the networks, **CMP-1-NH$_2$** was reacted with anhydrides of increasing chain lengths, up to hexanoic anhydride (**CMP-1-AMD5**; chain length = C_5). In all cases, yields of between 65 and 85% were calculated after washing with $CHCl_3$ to remove any unreacted anhydride. In all cases, FT-IR spectra showed the presence of the amide functionality at *ca.* 1680–1700 cm^{-1}. Elemental analysis shows a gradual decrease in nitrogen content from 2.27% for **CMP-1-AMD1** to 2.03% for **CMP-1-AMD5**, as expected, as the chain length increases (Table S1).

As the alkyl chain length in the amide is increased, the apparent BET surface area in the materials decreases systematically. **CMP-1-AMD5** shows the lowest surface area in the series (37 m^2/g, Fig. 4). The pore volume in the post-synthetically modified networks also decreases with increasing alkyl chain length, from 0.21 cm^3/g for **CMP-1-AMD1** to 0.04 for **CMP-1-AMD5**. The pore volumes at $P/P_0 = 0.1$ also show a systematic decrease from 0.12 to 0.01 cm^3/g. In fact, the microporosity of **CMP-1-AMD5** is almost completely removed by functionalisation with butyric anhydride. The ratio of microporosity, $V_{0.1/tot}$, also reduces with alkyl chain length, from 61% for **CMP-1-NH$_2$** to around 29% for **CMP-1-AMD5**. The calculated differential pore volumes (Fig. 5) show a decreasing in the pore volume of modified structures compared to **CMP-1-NH$_2$**, indicative of the pores in the network being filled by the amide group. The filling of pores is more pronounced for longer amide chain lengths, with **CMP-1-AMD5** having no pores less than 1 nm.

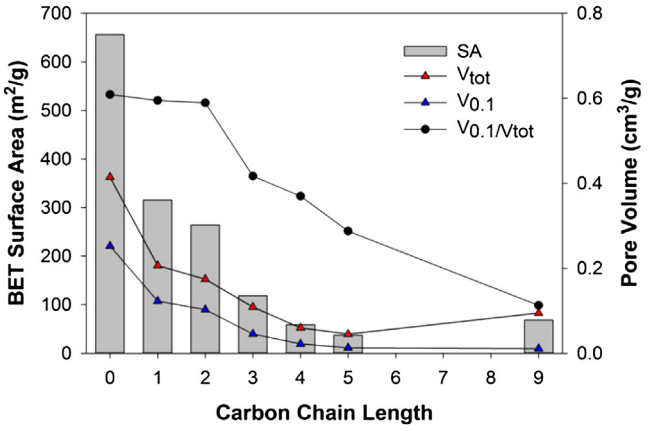

Fig. 4. BET surface areas, total (red triangles) and micropore volumes (blue triangles) and $V_{0.1/tot}$ (black circles) for **CMP-1-NH$_2$** and **CMP-1-AMDs 1-5** and **-9**. (For interpretation of the references to colour in this figure legend, the reader is referred to the web version of this article.)

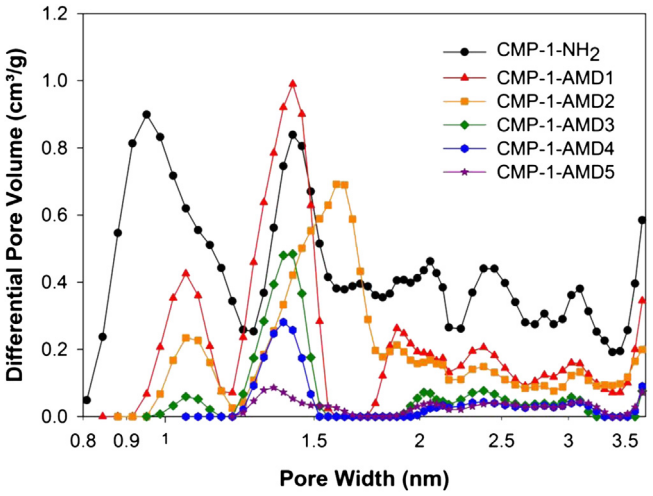

Fig. 5. NL-DFT pore size distributions.

We hypothesised that longer chain functionalisation may result in only the larger pores being accessible as have been suggested elsewhere [36]. To probe this, we synthesised **CMP-1-AMD9** by reaction of **CMP-1-NH$_2$** with decanoic anhydride. Amidation was again confirmed by the appearance of the amide C═O band at 1690 cm^{-1} in the IR spectrum. The conversion was again estimated from elemental analysis, and surprisingly was found to be higher than for the shorter chain examples. However, again we highlight the difficulties in using elemental analysis to calculate conversions. The calculated BET surface area of the PSM network was found to be 68 m^2/g, similar to **CMP-1-AMD4** and **CMP-1-AMD5**. However, this material was not microporous as can be seen from the nitrogen isotherm (Fig. S1) and calculated pore size distribution (Fig. S4). It therefore appears that this anhydride is still able to enter the pores, although it is also possible that the drop in porosity is due to the blockage of the larger pores at the surface of the material, and hence a reduction in accessibility to the smaller pores in the bulk solid.

It was also possible to modify **CMP-1-NH$_2$** with a chiral anhydride, (*S*)-(+)-2-methylbutyric anhydride. Previously, chirality has been difficult to achieve in CMPs, requiring the use of multistep monomer synthesis [45] or a simple chiral monomer which resulted however in a relatively low surface area network [46]. The primary chain length of the chiral amide is the same length as for **CMP-1-AMD3**. It might be expected therefore that the BET surface area and pore volume for the chiral network would be similar, and indeed the apparent BET surface area for the chiral network was calculated to be 226 m^2/g (*c.f.*, 119 m^2/g for **CMP-1-AMD3**). This surface area is also similar to that measured for a chiral binaphthalene polyimide [42]. The FT-IR of the chiral network shows a weaker amide bond (see Supporting Information Fig. S11) than seen for the linear amides. It is possible that the more bulky chiral amide is not able to functionalise as many of the amines in the network as the corresponding linear amides, and hence the conversion to the amide is lower, although absolute quantification was not possible by IR.

In order to determine if the tuneable pore sizes in these networks could be used to control the adsorption of gases, carbon dioxide isotherms were measured at 273 K and 298 K. As reported previously, **CMP-1-NH$_2$** had an uptake of 0.96 mmol/g at 298 K and 1.65 mmol/g at 273 K and 1 bar [7]. The amide-functionalised network, **CMP-1-AMD1**, adsorbed less CO_2 at 273 K (1.51 mmol) but similar amounts at 298 K (0.96 mmol/g). Further increases in the

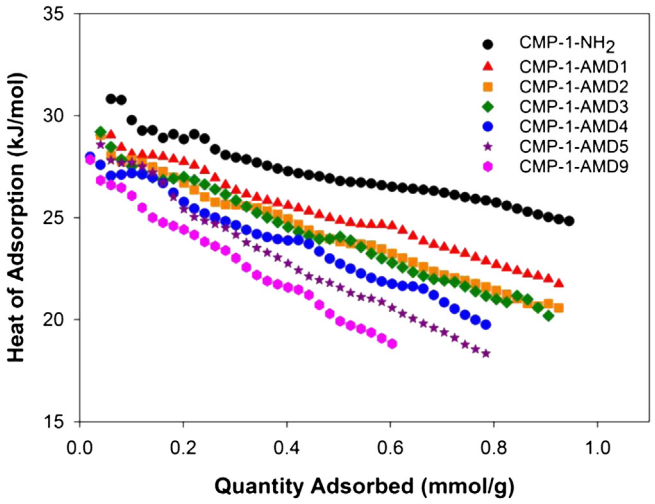

Fig. 6. Isosteric heats of adsorption for carbon dioxide.

amide chain length caused a further decrease in the quantity of CO_2 adsorbed from 0.92 mmol/g and 1.46 mmol/g for **CMP-1-AMD2** to 0.54 mmol/g and 0.87 mmol/g for **CMP-1-AMD9** at 298 K and 273 K, respectively. The decrease in the amount of CO_2 adsorbed correlates with the reduction of surface area and pore volumes. The isosteric heats of adsorption were calculated from the CO_2 isotherms collected at these two temperatures (Fig. 6). A reduction in isosteric heat was observed when going from the amine network to amides, and all networks showed decrease in isosteric heats as a function of increasing chain length. CO_2/N_2 selectivities for the networks at 298 K were also calculated by measuring the nitrogen isotherms at 298 K and using the Henry's law constants. In all cases, the CO_2/N_2 selectivity was between 8.5 and 12.0, a slight decrease from 14.6 for the parent **CMP-1-NH$_2$** (Table S2).

5. Conclusions

The post-synthetic amidation of CMPs has been demonstrated for the first time. Control over the pore sizes and absolute surface area is possible by amide formation using anhydrides with different chain lengths. Chirality can also be incorporated in a simple way without the need for complicated monomer synthesis. While the synthesis of microporous networks via metal-catalysed coupling chemistry allows the preparation of materials containing a wide range of functional groups [15,16], not all groups are necessarily tolerant to such metal catalysis routes. Hence, this post-functionalisation strategy offers the potential to extend the range of functionality in microporous polymers [38]. It has been shown elsewhere that post-functionalisation can be used to add a range of different functional groups to MOFs. It has also been shown that this strategy can be used to multiple substituents [39]. Such possibilities also exist for our polymers. Likewise the demonstration that pore sizes can be post-synthetically adjusted is interesting. The pore size distributions for MOPs tend to be broader than those for MOFs and other crystalline materials. Tuning post-synthetically may open up opportunities to tune broad pore sizes for specific applications, for example in adsorption and separations. In all of the above, we highlight that the post-synthetic modification approach should not be limited to amidation. Formation of imines for example has been shown for related networks [30]. Likewise, we have previously reported networks containing carboxylic acids, which are again amenable to this approach.

Acknowledgements

We thank the EPSRC and E.ON for funding (EP/G061785/1) through the E.ON-EPSRC strategic call on CCS. AIC is a Royal Society Wolfson Merit Award holder. TR thanks Mahidol University for funding.

Appendix A. Supplementary data

Supplementary data related to this article can be found at http://dx.doi.org/10.1016/j.polymer.2013.06.004.

References

[1] Dawson R, Cooper AI, Adams DJ. Prog Pol Sci 2011.
[2] McKeown NB, Budd PM. Macromolecules 2010;43:5163.
[3] Thomas A. Angew Chem Int Ed 2010;49:8328.
[4] Kaur P, Hupp JT, Nguyen ST. ACS Catal 2011;1:819.
[5] Budd PM, Butler A, Selbie J, Mahmood K, McKeown NB, Ghanem B, et al. Phys Chem Chem Phys 2007;9:1802.
[6] Dawson R, Stöckel E, Holst JR, Adams DJ, Cooper AI. Energy Env Sci 2011;4:4239.
[7] Jiang S, Bacsa J, Wu XF, Jones JTA, Dawson R, Trewin A, et al. Chem Commun 2011;47:8919.
[8] Dawson R, Cooper AI, Adams DJ. Polym Int 2013;62:345.
[9] Weber J, Thomas A. J Am Chem Soc 2008;130:6334.
[10] Chen L, Honsho Y, Seki S, Jiang DL. J Am Chem Soc 2010;132:6742.
[11] Jiang JX, Trewin A, Adams DJ, Cooper AI. Chem Sci 2011;2:1777.
[12] Kou Y, Xu Y, Guo Z, Jiang D. Angew Chem Int Ed 2011;50:8753.
[13] Budd PM, McKeown NB. Polym Chem 2010;1:63.
[14] Jiang J-X, Cooper A. Top Curr Chem 2010;293:1.
[15] Dawson R, Laybourn A, Clowes R, Khimyak YZ, Adams DJ, Cooper AI. Macromolecules 2009;42:8809.
[16] Dawson R, Laybourn A, Khimyak YZ, Adams DJ, Cooper AI. Macromolecules 2010;43:8524.
[17] Ben T, Ren H, Ma SQ, Cao DP, Lan JH, Jing XF, et al. Angew Chem Int Ed 2009;48:9457.
[18] Holst JR, Cooper AI. Adv Mater 2010;22:5212.
[19] Yuan D, Lu W, Zhao D, Zhou H-C. Adv Mater 2011;23:3723.
[20] Wang Z, Cohen SM. Chem Soc Rev 2009;38:1315.
[21] Cooper AI. Adv Mater 2009;21:1291.
[22] Stöckel E, Wu XF, Trewin A, Wood CD, Clowes R, Campbell NL, et al. Chem Commun 2009:212.
[23] Jiang J-X, Su F, Trewin A, Wood CD, Niu H, Jones JTA, et al. J Am Chem Soc 2008;130:7710.
[24] Dawson R, Adams DJ, Cooper AI. Chem Sci 2011;2:1173.
[25] Zhang Y, Zhang Y, Sun YL, Du X, Shi JY, Wang WD, et al. Chem Eur J 2012;18:6328.
[26] Cohen SM. Chem Sci 2010;1:32.
[27] Tanabe KK, Cohen SM. Chem Soc Rev 2011;40:498.
[28] Ingleson MJ, Perez Barrio J, Guilbaud J-B, Khimyak YZ, Rosseinsky MJ. Chem Commun 2008:2680.
[29] Du N, Park HB, Robertson GP, Dal-Cin MM, Visser T, Scoles L, et al. Nat Mater 2011;10:372.
[30] Kerneghan PA, Halperin SD, Bryce DL, Maly KE. Can J Chem 2011;89:577.
[31] Weber J, Du N, Guiver MD. Macromolecules 2011;44:1763.
[32] Du N, Robertson GP, Song J, Pinnau I, Guiver MD. Macromolecules 2009;42:6038.
[33] Jiang J-X, Wang C, Laybourn A, Hasell T, Clowes R, Khimyak YZ, et al. Angew Chem Int Ed 2011;50:1072.
[34] Bunck DN, Dichtel WR. Chem Commun 2013;49:2457.
[35] Urakami H, Zhang K, Vilela F. Chem Commun 2013;49:2353.
[36] Kiskan B, Weber J. ACS Macro Lett 2012;1:37.
[37] Mohanty P, Kull LD, Landskron K. Nat Commun 2011;2:401.
[38] Wang Z, Tanabe KK, Cohen SM. Inorg Chem 2009;48:296.
[39] Garibay SJ, Wang Z, Tanabe KK, Cohen SM. Inorg Chem 2009;48:7341.
[40] Jiang JX, Su F, Trewin A, Wood CD, Campbell NL, Niu H, et al. Angew Chem Int Ed 2007;46:8574.
[41] Jiang JX, Laybourn A, Clowes R, Khimyak YZ, Bacsa J, Higgins SJ, et al. Macromolecules 2010;43:7577.
[42] Tanabe KK, Wang Z, Cohen SM. J Am Chem Soc 2008;130:8508.
[43] Tilford RW, Mugavero SJ, Pellachia PJ, Lavigne JL. Adv Mater 2008;20:2741.
[44] Ghanem BS, Hashem M, Harris KDM, Msayib KJ, Xu M, Budd PM, et al. Macromolecules 2010;43:5287.
[45] Ma L, Wanderley MM, Lin W. ACS Catal 2011;1:691.
[46] Ritter N, Senkovska I, Kaskel S, Weber J. Macromol Rapid Commun 2011;32:438.